

Investigation on phase noise of the signal from a singly resonant optical parametric oscillator

Feng Jinxia^{1,2}, Li Yuanji^{1,2} and Zhang Kuanshou^{1,2}

¹ State Key Laboratory of Quantum Optics and Quantum Optics Devices, Institute of Opto-Electronics, Shanxi University, Taiyuan 030006, People's Republic of China

² Collaborative Innovation Centre of Extreme Optics, Shanxi University, Taiyuan, Shanxi 030006, People's Republic of China

E-mail: kuanshou@sxu.edu.cn

Accepted for publication 8 January 2018

Published 28 February 2018



CrossMark

Abstract

The phase noise of the signal from a singly resonant optical parametric oscillator (SRO) is investigated theoretically and experimentally. An SRO based on periodically poled lithium niobate is built up that generates the signal with a maximum power of 5.2 W at 1.5 μm . The intensity noise of the signal reaches the shot noise level for frequencies above 5 MHz. The phase noise of the signal oscillates depending on the analysis frequency, and there are phase noise peaks above the shot noise level at the peak frequencies. To explain the phase noise feature of the signal, a semi-classical theoretical model of SROs including the guided acoustic wave Brillouin scattering effect within the nonlinear crystal is developed. The theoretical predictions are in good agreement with the experimental results.

Keywords: optical parametric oscillators, phase noise of the signal, guided acoustic wave Brillouin scattering effect

(Some figures may appear in colour only in the online journal)

1. Introduction

Optical parametric oscillators (OPOs) are a mature technology for generating tunable coherent radiation in various spectral domains from the visible to terahertz [1, 2]. In particular, the singly resonant OPO (SRO) possesses several advantages, such as high power, continuous wavelength tuning capability, and good power stability [3, 4]. Since the laser source generated by a continuous wave (cw) OPO can be applied to the research of quantum information processing [5, 6], it is crucial to investigate the excess noise of the output from SROs. The additional phase noise was observed in triply resonant OPOs based on KTiOPO_4 (KTP) crystal and explained theoretically by a thermal phonon model that considers a random local fluctuation in permittivity of KTP crystal [7]. However,

investigations on the phase noise of SROs based on periodically poled nonlinear crystal are rare, while the intensity noise has been observed in numerous experiments [8–10].

The performances of entanglements from second-harmonic generation or degenerate OPOs are also limited by excess phase noise. The phase quadrature spectrum observed consists of a set of narrow peaks above the shot noise level (SNL) [11, 12]. A likely explanation is that the guided acoustic wave Brillouin scattering (GAWBS) occurs within the nonlinear crystal [12]. The acoustic elastic modes (AEMs) of the crystal are excited by the thermal energy of the crystal, and the standing pressure waves caused by AEMs modulate the phase of light throughout the crystal. In fact, the model was proposed initially to explain the excess phase noise for light transmitting through the optical fibre, where the thermal fluctuations of refractive index in the fibre cause the optical field to acquire phase noise sidebands [13, 14].

In this letter, an SRO based on periodically poled lithium niobate (PPLN) is constructed and noise spectra of the signal



Original content from this work may be used under the terms of the [Creative Commons Attribution 3.0 licence](https://creativecommons.org/licenses/by/3.0/). Any further distribution of this work must maintain attribution to the author(s) and the title of the work, journal citation and DOI.

from the SRO are investigated experimentally. A semi-classical theoretical model of SROs including the GAWBS effect within the nonlinear crystal is developed to explain the phase noise feature of the signal. The influences of SRO parameters on the phase noise of the signal are discussed in detail.

2. Theoretical description

Figure 1 shows a schematic of an SRO such that only the signal is resonated in the cavity; the pump double-passes through the crystal and the idler is not reflected at all on the cavity mirrors.

In this system, the equation of motion for the signal field in the cavity is [15]:

$$\tau \dot{\alpha}_2 + \gamma'_2 \alpha_2 = 2\chi \alpha_0 \alpha_1^* + 2\chi \alpha'_0 \alpha_1'^* + \sqrt{2\gamma_2} \alpha_{2,\text{in}} + \sqrt{2\mu_2} \beta_{2,\text{in}}, \quad (1)$$

where α_i ($i = 0, 1, 2$) denote the pump, idler, and signal fields respectively; τ is the cavity round-trip time; and γ_2 is the round-trip loss parameter of the signal related to the output coupling transmission. μ_2 is the other loss parameter of the signal (such as crystal absorption, surface scattering, and imperfections of mirrors). γ'_2 is the total loss coefficient, defined as $\gamma'_2 = \gamma_2 + \mu_2$. χ is the second-order nonlinear coefficient of the crystal. $\alpha_{2,\text{in}}$, $\alpha'_{2,\text{in}}$ and $\beta_{2,\text{in}}$ are the incoming signal fields, associated with the input coupler, output coupler and the internal loss mechanism, respectively. α_0 (α'_0) and α_1 (α'_1) denote the forward (backward) pump and idler fields in the middle of the crystal, respectively. $\alpha_i(L)$ and $\alpha'_i(L)$ represent the forward and backward fields at the exits of the crystal. L is the length of the crystal. The fields can be expressed as the following set of equations:

$$\begin{cases} \alpha_0 = \alpha_{0,\text{in}} - \chi \alpha_1 \alpha_2 & \alpha'_0 = \alpha_0(L) - \chi \alpha'_1 \alpha_2 \\ \alpha_0(L) = \alpha_{0,\text{in}} - 2\chi \alpha_1 \alpha_2 & \alpha'_0(L) = \alpha_0(L) - 2\chi \alpha'_1 \alpha_2 \\ \alpha_1 = \chi \alpha_0 \alpha_2^* & \alpha'_1 = \chi \alpha'_0 \alpha_2^* \\ \alpha_1(L) = 2\chi \alpha_0 \alpha_2^* & \alpha'_1(L) = 2\chi \alpha'_0 \alpha_2^* \end{cases}, \quad (2)$$

where $\alpha_{0,\text{in}}$ is the input pump field. Therefore, the classical and quantum fluctuation characterization can be obtained by the evolution of the coupled fields in equations (1) and (2) and using a linearized description of the fields:

$$\alpha_i = \bar{\alpha}_i + \delta\alpha_i. \quad (3)$$

The signal power from the SRO can be calculated by taking $\alpha_{2,\text{in}} = \beta_{2,\text{in}} = 0$:

$$P_{\text{out}} = |\bar{\alpha}_{2,\text{out}}|^2 = 2\gamma_2 \bar{\alpha}_2^2, \quad (4)$$

and the pump threshold can be written by:

$$P_{\text{th}} = \gamma'_2 / 4\chi^2. \quad (5)$$

The amplitude and phase fluctuations of the fields can be defined by:

$$\delta X_i = \delta\alpha_i + \delta\alpha_i^*, \quad \delta Y_i = -i(\delta\alpha_i - \delta\alpha_i^*). \quad (6)$$

The phase fluctuation equations of motion of the signal can be written as:

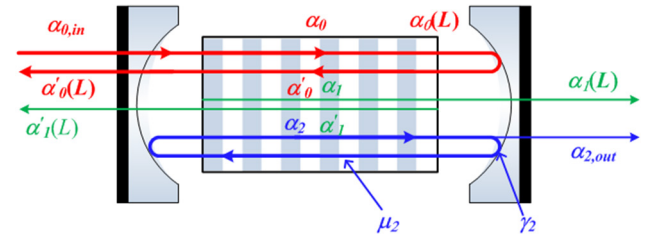


Figure 1. Schematic of an SRO with only signal resonated in the cavity.

$$\begin{aligned} \delta \dot{Y}_2 = & -(\gamma'_2 + 2\mu\bar{\alpha}_2^2)\delta Y_2 - (\sqrt{2\mu}\bar{\alpha}_{0,\text{in}} - \mu\bar{\alpha}_2^2)\delta Y_2 \\ & + 2\sqrt{\mu}\bar{\alpha}_2\delta Y_{0,\text{in}} + \sqrt{2\gamma_2}\delta Y_{\alpha_{2,\text{in}}} + \sqrt{2\mu_2}\delta Y_{\beta_{2,\text{in}}}, \end{aligned} \quad (7)$$

where $\mu = \hbar\omega\gamma_{\text{sh}}/2\tau^2$ is defined as the two photon damping rate, ω is the angular frequency of the signal, γ_{sh} is the second-harmonic photon loss rate which is related to the characteristics of the crystal.

The phase noise spectrum can be obtained by means of a Fourier transform of equation (7). To investigate the excess phase noise of the signal from the SRO, we extend the model to include the GAWBS effect within the nonlinear crystal, the phase fluctuation of the signal can be given by:

$$\delta Y_2 = \frac{2\sqrt{\mu}\bar{\alpha}_2\delta Y_{0,\text{in}} + \sqrt{2\gamma_2}\delta Y_{\alpha_{2,\text{in}}} + \sqrt{2\mu_2}\delta Y_{\beta_{2,\text{in}}} + \delta Q_G}{\gamma'_2 + \mu\bar{\alpha}_2^2 + \sqrt{2\mu}\bar{\alpha}_{0,\text{in}} - i2\pi\Omega}, \quad (8)$$

where δQ_G is the fluctuation induced by GAWBS, Ω is the analysis frequency.

Using the input–output relation of the signal from the SRO

$$\delta Y_{2,\text{out}} = \sqrt{2\gamma_2}\delta Y_2 - \delta Y'_{\alpha_{2,\text{in}}}, \quad (9)$$

and assuming that the pump and incoming signal fields and noise of extra losses are uncorrelated and coherent with variance of 1, the phase noise spectrum of the output field of the signal can be obtained as:

$$S(\Omega) = \langle |\delta Y_{2,\text{out}}|^2 \rangle = 1 - \frac{4(\sigma - \mu\bar{\alpha}_2^2/\gamma'_2 - V_{Q_G}/\gamma'_2)}{(1 + \mu\bar{\alpha}_2^2/\gamma'_2 + \sigma)^2 + \Omega_c^2}, \quad (10)$$

where $\Omega_c = \Omega/\gamma'_2$ is the normalized analysis frequency. $\sigma = \alpha_{0,\text{in}}/\alpha_{\text{th}}$ is the pump ratio. The phase fluctuation V_{Q_G} induced by GAWBS is given by [12]:

$$V_{Q_G} = \sqrt{2\eta_G}\bar{\alpha}_2, \quad (11)$$

where $\eta_G = (\varphi/2)^2$ is the Brillouin scattering efficiency, and $\varphi = \frac{2\pi L}{\lambda}\Delta n$ is the phase shift caused by the change of the refractive index of nonlinear crystal (Δn). Δn is induced by AEM that is related to the nonlinear crystal temperature and the modulation frequency. λ is the wavelength of the signal.

3. Experimental setup and results

The experimental setup of the SRO based on PPLN is schematized in figure 2. The pump source is a homemade stable cw single-frequency Nd:YVO₄ laser at 1.064 μm [16] with a

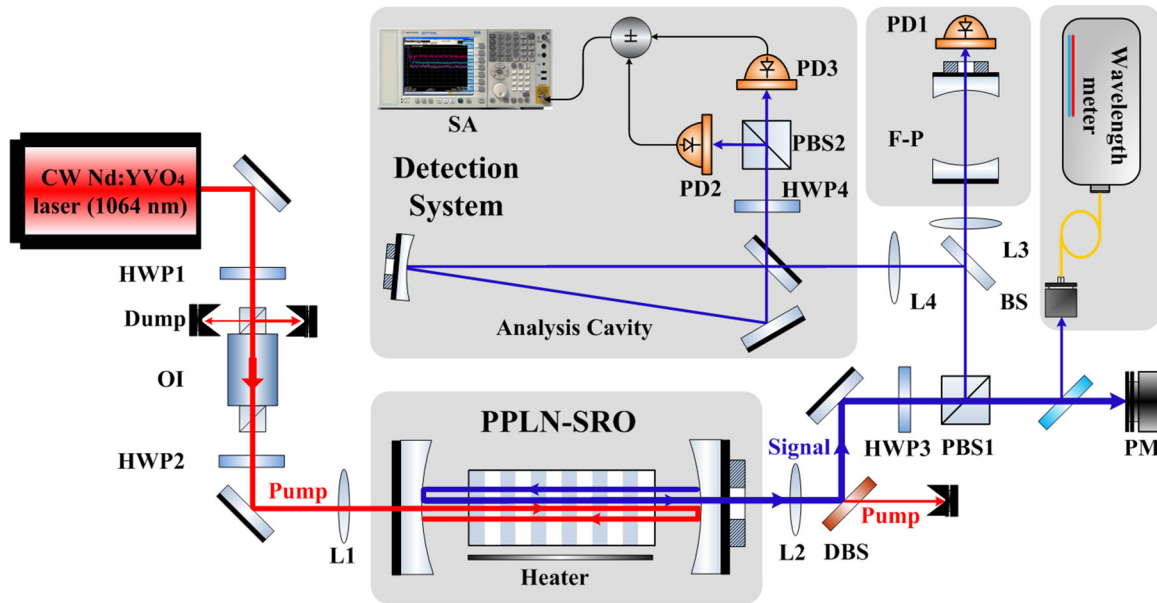


Figure 2. Experimental setup of the SRO based on PPLN. HWP: half-wave plate; OI: optical isolator; PBS: polarising beam splitter; DBS: dichroic beam splitter; PM: power meter; SA: spectrum analyser; PD: photo detector.

maximum output of 22 W and mode hopping-free operation. The SRO is a linear cavity comprising two concave mirrors with a curvature radius of 26 mm and a PPLN crystal. The input coupler has high reflectivity ($R > 99.8\%$) over $1.5 \mu\text{m}$ – $1.65 \mu\text{m}$ and high transmission ($T > 95\%$) at $1.064 \mu\text{m}$. The output coupler has high reflectivity ($R > 99.9\%$) at $1.064 \mu\text{m}$ and partial transmission over $1.5 \mu\text{m}$ – $1.65 \mu\text{m}$ to extract the signal. The host material of the couplers is BK7 glass, which is not transparent to light at wavelengths around $3.3 \mu\text{m}$, so the idler is not extracted from the SRO in our experiment. The PPLN crystal, with dimensions of 30 mm (length) \times 10 mm (width) \times 1 mm (thickness) and a poling period of $29.8 \mu\text{m}$, is housed in a copper oven and temperature-controlled by a home-made temperature controller with an accuracy of $0.004 \text{ }^\circ\text{C}$. The SRO cavity length is set as 64 mm, and the free spectral range of the SRO cavity is about 1.5 GHz. The pump beam is focused via a lens (L1) to a spot with radius of about $49 \mu\text{m}$ at the center of the PPLN crystal. The mode match of the pump was achieved, and the mode overlap between the pump beam and signal mode was 0.68.

The signal power was measured using a power meter (LabMax-TOP, Coherent), while the longitudinal mode was monitored using a scanning confocal Fabry–Perot (F–P) interferometer. The wavelength of the signal was measured using a wavelength meter with a resolution of 0.1 pm (WS/6-771, HighFinesse). The signal wavelength can be tuned from $1.56 \mu\text{m}$ to $1.59 \mu\text{m}$ when the PPLN temperature is controlled from $120 \text{ }^\circ\text{C}$ to $180 \text{ }^\circ\text{C}$.

Figure 3 shows the extracted signal power versus pump power when the 1.8% output coupler is used and the PPLN temperature is controlled to $120 \text{ }^\circ\text{C}$. The blue balls in figure 3 are the experimental results. The red solid curve is the theoretical prediction using equations (4) and (5). A pump threshold as low as 2.5 W was achieved, a signal with a power of 5.2 W

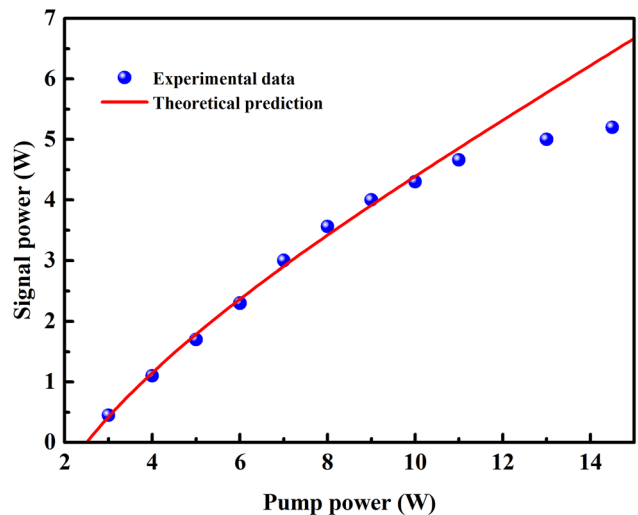


Figure 3. Signal power as a function of pump power.

was obtained at a pump power of 14.5 W, and the SRO could maintain single-frequency operation over the whole pump range. The long-term power stability was better than $\pm 1\%$ over a period of 2 h. As mentioned in the experimental setup, the host material of the couplers is BK7 glass and the idler around $3.3 \mu\text{m}$ was not extracted from the SRO. The estimated idler output power is about 2 W, no destruction of the mirror was observed in our experimental even if the idler is fully absorbed in BK7 glass.

During our experiment, a small part of the signal with power P_{det} was used to investigate the noise of the signal from the SRO. A self-homodyne-detection system composed of HWP4, PBS2, and two photo-detectors, PD2 and PD3 (ETX-300, Epitaxx), was used to measure the intensity noise of the signal directly. The measurement of phase noise was performed using the ellipse rotation method described in [17],

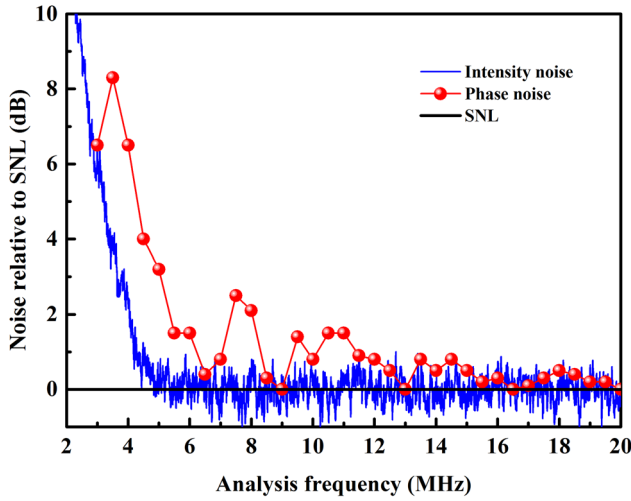


Figure 4. Measured intensity and phase noise spectra of signal relative to SNL.

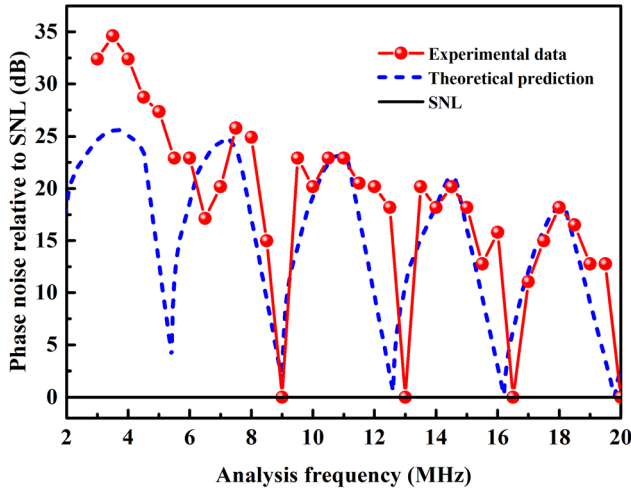


Figure 5. Phase noise spectra of signal relative to SNL.

with the help of an analysis cavity. The analysis cavity has a finesse of 105 and bandwidth of 1.4 MHz, allowing for a complete conversion of the phase noise to intensity noise for frequencies above 2 MHz. The measured noise spectra were recorded using a spectrum analyzer (N9010A, Agilent) with a resolution bandwidth of 100 kHz, a video bandwidth of 300 Hz, and a sweep time of 1 s.

Figure 4 shows the measured intensity and phase noise spectra of signal relative to SNL at $P_{\text{det}} = 16$ mW when the signal power was 4 W and the PPLN temperature was 130 °C. It can be seen that the intensity noise (the blue curve) reaches the SNL for frequencies above 5 MHz, which performed similar feature of pump [16]. This indicates the signal intensity noise is mainly caused by the transferred noise from pump. However, a number of frequency-dependent excess phase noise peaks exist above the SNL (the red balls) over the frequency range from 2 MHz to 20 MHz, which is absent in the phase noise of the pump [16]. The excess phase noise is

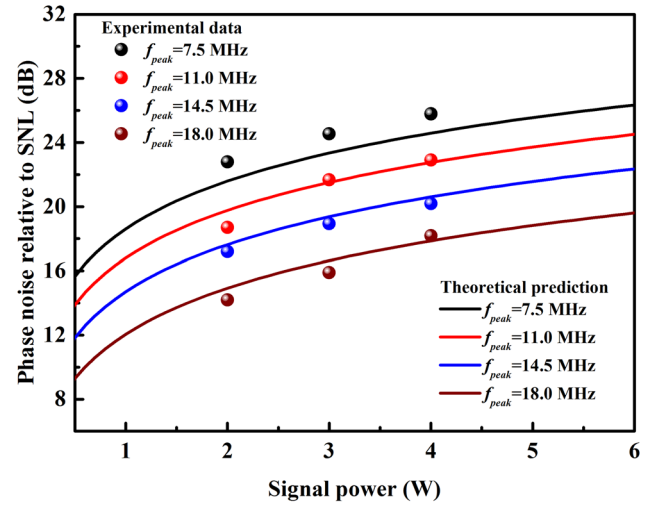


Figure 6. Phase noise of signal versus signal power at different peak frequencies.

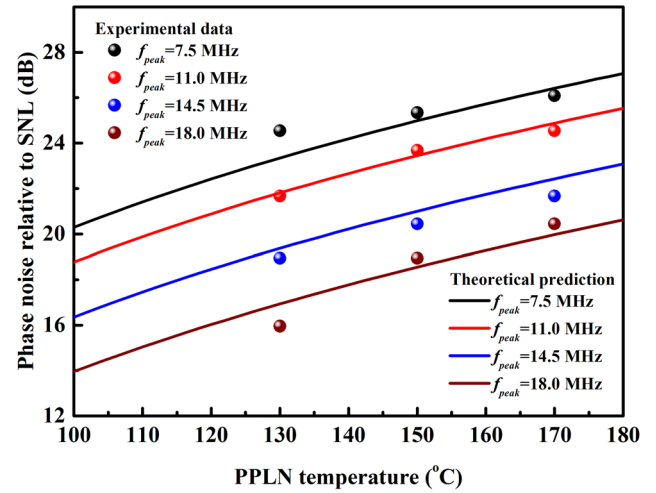


Figure 7. Phase noise of signal versus PPLN temperature at different peak frequencies.

caused by the GAWBS effect in the nonlinear crystal that will be discussed in the following section.

4. Discussion

To discuss the performance of the signal phase noise, the measured noise spectrum (S_{mea}) when signal power is attenuated to P_{det} should be converted to the actual one (S_{act}) with the signal power of P_{out} , using the relationship [18]:

$$S_{\text{act}} = \frac{P_{\text{out}}}{P_{\text{det}}} (S_{\text{mea}} - 1) + 1. \quad (12)$$

The theoretical prediction of the phase noise calculated using equation (10) is compared with the actual phase noise of the signal, as shown in figure 5. The red balls are the actual phase noise converted by the measured one in figure 4 using equation (12). The dashed curve is the theoretical prediction that considers the influence of the GAWBS effect with the

parameters of $\sigma = 1.9$, $\gamma'_2 = 0.015$. It can be seen that the phase noise of the signal oscillates depending on the analysis frequency, and there are phase noise peaks above the SNL at the peak frequencies (f_{peak}), such as 7.5 MHz, 11 MHz, 14.5 MHz, and 18 MHz. The discrepancy between theory and experiment for frequencies below 6 MHz is due to there being excess intensity noise from the pump. The excess intensity noise of the pump can be transferred to the phase noise of the signal, but is not considered in our numerical simulations.

The measured and calculated signal phase noises' dependences on the signal power at different f_{peak} values, when PPLN temperature was 130 °C, are shown in figure 6. It can be seen that the phase noise of the signal increases with increasing signal power. Meanwhile, we investigated the phase noise of the signal at different transmissions of output coupler and constant signal power. We found that the phase noise of the signal is not dependent on the transmission of the output coupler. This result indicates that the phase noise is irrelevant to the linewidth of the SRO cavity.

Figure 7 shows the PPLN temperature dependence of the signal phase noise at different f_{peak} values when the signal power was 3 W. We can see that the phase noise of the signal decreases with decreasing PPLN temperature. The results indicate that the excess phase noise can be reduced using nonlinear crystals with a lower work temperature, such as MgO-doped PPLN crystal.

5. Conclusions

We investigated the noise of the signal from an SRO theoretically and experimentally. The SRO is built up based on PPLN and pumped by a homemade stable cw single-frequency Nd:YVO₄ laser. A cw single-frequency signal at 1.5 μm is generated, with a maximum output power of 5.2 W. The intensity noise of the signal reaches the SNL for frequencies above 5 MHz. The phase noise of the signal oscillates depending on the analysis frequency, and there are excess phase noise peaks above the SNL at the peak frequencies. The excess phase noise of the signal depends on the PPLN temperature and signal power. To explain the phase noise feature of the signal, we extend the semi-classical theoretical model of SROs to include the GAWBS effect within the nonlinear crystal. The theoretical predictions are in good agreement with the experimental results.

Acknowledgments

This research was supported by National Key R&D Program of China (NO. 2016YFA0301401) and sponsored by the Fund for Shanxi '1331 Project' Key Subjects Construction (1331KS).

References

- [1] Wang P, Shang Y, Li X, Shen M and Xu X 2017 *Laser Phys. Lett.* **14** 025401
- [2] Kostyukova N Y, Kolker D B, Zenov K G, Boyko A A, Starikova M K, Sherstov I V and Karapuzikov A A 2015 *Laser Phys. Lett.* **12** 095401
- [3] Zeil P, Thilmann N, Pasiskevicius V and Laurell F 2014 *Opt. Express* **22** 29907–13
- [4] Kumar S C, Das R, Samanta G K and Ebrahim-Zadeh M 2011 *Appl. Phys. B* **102** 31–5
- [5] Laurat J, Coudreau T, Treps N, Maître A and Fabre C 2003 *Phys. Rev. Lett.* **91** 213601
- [6] Mehmet M, Ast S, Eberle T, Steinlechner S, Vahlbruch H and Schnabel R 2011 *Opt. Express* **19** 25763–72
- [7] César J E S, Coelho A S, Cassemiro K N, Villar A S, Lassen M, Nussenzveig P and Martinelli M 2009 *Phys. Rev. A* **79** 063816
- [8] Mhibik O, My T H, Paboeuf D, Bretenaker F and Drag C 2010 *Opt. Lett.* **35** 2364–6
- [9] Mhibik O, Paboeuf D, Drag C and Bretenaker F 2011 *Opt. Express* **19** 18049–57
- [10] Li P, Li Y and Zhang K 2015 *Laser Phys. Lett.* **12** 045401
- [11] Grosse N B, Assad S, Mehmet M, Schnabel R, Symul T and Lam P K 2008 *Phys. Rev. Lett.* **100** 243601
- [12] Grosse N B 2009 *PhD Thesis* The Australian National University, Australia pp 162–5 (available at: <http://photonics.anu.edu.au/theses/Thesis%20ANU%20PhD%202009%20Grosse.pdf>)
- [13] Shelby R M, Levenson M D and Bayer P W 1985 *Phys. Rev. Lett.* **54** 939–42
- [14] Poustie A J 1993 *J. Opt. Soc. Am. B* **10** 691–6
- [15] Fabre C, Giacobino E, Heidmann A and Reynaud S 1989 *J. Phys. France* **50** 1209–25
- [16] Liu Q, Liu J L, Jiao Y C, Li P, Feng J X and Zhang K S 2012 *Chin. Phys. Lett.* **29** 054205
- [17] Villar A S, Martinelli M and Nussenzveig P 2004 *Opt. Commun.* **242** 551–63
- [18] Harb C C, Ralph T C, Huntington E H, Freitag I, McClelland D E and Bachor H 1996 *Phys. Rev. A* **54** 4370–82